HHS Public Access

Author manuscript

Dev Neurosci. Author manuscript; available in PMC 2022 March 03.

Published in final edited form as:

Dev Neurosci. 2020 ; 42(5-6): 195–207. doi:10.1159/000513536.

Integrated RNA sequencing reveals epigenetic impacts of diesel particulate matter exposure in human cerebral organoids

Stephanie M. Bilinovich[a], **Katie L Uhl**[a], **Kristy Lewis**[a], **Xavier Soehnlen**[a], **Michael Williams**[a,b,c], **Daniel Vogt**[a,b,c], **Jeremy W. Prokop**[a,b,d,*], **Daniel B. Campbell**[a,b,c,*]

[a]Department of Pediatrics & Human Development, Michigan State University, Grand Rapids, MI. 49503

[b]Center for Research in Autism, Intellectual, and other Neurodevelopmental Disabilities, Michigan State University, East Lansing, MI, 48824, USA

[c]Neuroscience Program, Michigan State University, East Lansing, MI, 48824, USA

[d]Department of Pharmacology and Toxicology, Michigan State University, East Lansing, MI, 48824, USA

Abstract

Autism Spectrum Disorder (ASD) manifests early in childhood. While genetic variants increase risk for ASD, a growing body of literature has established that *in utero* chemical exposures also contribute to ASD risk. These chemicals include air-based pollutants like diesel particulate matter (DPM). A combination of single-cell and direct transcriptomics of DPM exposed human induced pluripotent stem cell derived cerebral organoids, reveal toxicogenomic effects of DPM exposure during fetal brain development. Direct transcriptomics, sequencing RNA bases via Nanopore, revealed that cerebral organoids contain extensive RNA modifications, with DPM altering cytosine methylation in oxidative mitochondrial transcripts expressed in outer radial glia cells. Single-cell transcriptomics further confirmed an oxidative phosphorylation change in cell groups such as outer radial glia upon DPM exposure. This approach highlights how DPM exposure perturbs normal mitochondrial function and cellular respiration during early brain development, which may contribute to developmental disorders like ASD by altering neurodevelopment.

Keywords

Autism; cerebral organoids; transcriptomics; epigenetics; diesel particulate matter

*Corresponding Authors: Jeremy W Prokop (jprokop54@gmail.com), Tel: 616-234-2889, Daniel B Campbell (campb971@msu.edu), 400 Monroe Ave NW, Grand Rapids MI 49503 USA, Tel: 616-234-2636.

Author Contributions

Performed experiments (SMB, KLU, KL, DV), analyzed data (SMB, DV, MW, JWP, DBC), designed experiments (SMB, DV, JWP, DBC), wrote the manuscript (SMB, JWP, DBC). All authors have read and approve of the manuscript.

Conflict of Interest Statement

The authors have no conflicts of interest to declare.

Introduction

It has long been hypothesized that environmental conditions during fetal *in utero* development can have physiological impacts on health from childhood into adulthood[1,2]. Environmental conditions shown to have impacts on developmental health include pollution, malnutrition, chemical, and viral exposures (i.e. Zika)[3]. Diesel particulate matter (DPM) is a major component of air pollution, originating from truck exhaust. Prenatal DPM exposure has been linked to glucose dysregulation in early childhood[4], low birth weight[5], preterm birth, and autism spectrum disorders[6]. However, few molecular mechanisms and the involvement of specific cell types have been proposed for the DPM exposure risk to date.

In addition to DPM exposure, many additional environmental toxicants are known to correlate with neurological and behavioral problems if exposures occur *in utero*. These pollutants include lead[7], ethanol[8], polycyclic aromatic hydrocarbons (PAHs)[9], and polybrominated diphenyl ether (PBDE) flame retardants[10]. Most studies into neurotoxicants and the effects on the developing brain are either animal studies or epidemiological cohort studies. While epidemiological studies are key in identifying neurotoxic effects in children, these studies lack the ability to implicate the molecular changes that may give rise to the neurological disorders. Animal studies can help to elucidate these molecular changes during prenatal development and are important tools in studying molecular mechanisms; however, there are disadvantages to using animal models for neurodevelopmental disorders. Rodent cerebral cortices are smooth (lissencephalic), whereas human cerebral cortex is composed of complex folding (gyrencephalic), with critical differences in the neural migrations that occur in early development[11,12]. Long noncoding RNAs (lncRNASs) are increased in both number and abundance in human brain cerebral cortex compared to rodents, indicating increased molecular complexity[13]. Single-cell transcriptomics of human and mouse midbrain development have shown similar cell groups but have several key differences[14,15]. With an interest in ASD risk factors, like DPM exposure on the developing cerebral cortex, human models present advantages over rodent models.

To overcome the limitations of rodent models in examining human genetics, recent advances in induced pluripotent stem cells (iPSCs) and human cerebral organoid cultures[16] have made it possible to study environmental exposures for toxicogenomics[17]. Cerebral organoids are a 3-dimensional cell culture that allows for a model of human embryonic brain development with multiple neural cell types. Not only do cerebral organoids mimic human development, but they can be scaled for use in cutting edge transcriptomic technologies like directly sequencing RNA transcripts for the detection of RNA base modifications transcriptome wide. In this paper we used cerebral organoids exposed to DPM in conjunction with ribosomal reduced RNAseq, direct and PCR amplified Nanopore sequencing, and single-cell (sc)-RNA sequencing to investigate DPM induced changes that occur during early brain development, lending insights into the toxicogenomic effects of air pollution on childhood neurodevelopmental disorders (Fig. 1).

Materials and Methods

Human iPSC Cell Lines

Four cell lines were used throughout this manuscript. Three lines were purchased from the iPSC Repository Catalog at California's Stem Cell Agency (CIRM): Line A (CW20050, male proband with ASD), Line B (CW20047, male brother of Line A without ASD), Line C (CW20012, female sister of Line A with ASD). A fourth line was obtained from the Allen Brain Atlas (AICS-0011, male without ASD) and was used for the bulk of experiments. Using line AICS-0011, four stable knockdown lines were created using prepackaged Mission shRNA lenti particles (GATAD2B- TRCN0000015317, CHD8-TRCN0000367896, TSC2- TRCN0000040182, ASXL3- TRCN0000246267) followed by selection with Puromycin. All iPSCs were cultured on StemAdhere or Vitronectin XF (Nucleus Biologics) in mTeSR1 media (StemCell Technology) at 37°C with 5% CO_2.

Cerebral Organoid Generation

Cerebral organoids were generated using the STEMdiff™ Cerebral Organoid Kit (STEMCELL Technologies, #08570). In brief, iPSC lines were grown until they reached approximately 80% confluency with minimal evidence of scaffolding. Cells were lifted from the plate using Gentle Cell Dissociation Reagent (STEMCELL Technologies, #07174) and plated onto round bottom ultra-low attachment 96-well plates (Corning, #7007) at a density of 9,000 cells/per well. Embryoid bodies were transferred into ultra-low attachment 24-well plates (Corning, #3473). On Day 8, embryoid bodies were embedded in Matrigel® (Corning, #354277) and transferred to ultra-low attachment 6-well plates (STEMCELL Technologies, #27145). Three days after embedding, organoids were transferred to a CO2 Resistant Shaker (ThermoFisher, # 88881102) set to 75 rpm. Media was changed every 2–3 days until the organoids reached Day 40 of maturation or treatment.

Organoid Exposure

On day 30 of the organoid maturation protocol, organoids were treated with an environmental toxicant for 7 days. Media was changed every 2 days. Treatments included to a final concentration: Phosphate buffered saline (PBS), 30mg DPM dissolved in PBS, 30μg DPM + 0.5% dimethyl sulfoxide (DMSO), 1% ethanol, and 0.5% DMSO.

RNA Isolation and Quality Control

When the cerebral organoids reached Day 37–40 of maturation the RNA was isolated using the QIAshredder (QIAGEN, #79656) and RNeasy Mini Kit (QIAGEN, #74104), pooling 30–40 cerebral organoids per column for the direct or PCR amplified nanopore sequencing and using a single organoid per column for ribosomal reduced RNAseq. RNA was isolated from 6 DPM exposed organoids and 6 PBS treated organoids, with each organoid treated as its own sample for ribosomal reduced RNAseq. RNA for all experiments was quantified using the Qubit™ RNA BR Assay Kit (Invitrogen, # Q10210) and assessed using the 5200 Fragment Analyzer System with the RNA Kit (Agilent, #DNF-471-0500).

Ribosomal reduced RNAseq and Bioinformatics

The isolated RNA from the DPM and PBS exposed organoids were submitted to the Van Andel Institute genomics core for library preparation and RNA-sequencing. Library was prepared with TruSeq RNA library Prep Kit v2 (Illumina) and sequencing on the Illumina NextSeq 500. FASTQ files (PRJNA640661) were processed using SALMON[18] using Gencode v.30. Aligned reads were analyzed for differential expression with DESeq2 (qVal < 0.05) [19].

Nanopore Sequencing and Bioinformatics

PCR amplified RNAseq of the 12 organoid samples (4 different iPSC cell lines, and different chemical exposures) was performed using cDNA-PCR sequencing kit and protocol (Oxford Nanopore Technologies, #SQK-PCS109) using 50 ng total RNA, Maxima H Minus Reverse Transcriptase (ThermoFisher Scientific, #EP0751), 2X LongAmp Taq Master Mix (NEB, #M0287), NEB Exonuclease (NEB, #M0293) and purified with Agencourt AMPure XP beads (Beckman Coulter, #A63881). Direct RNAseq on the samples (2 DPM exposed organoid rounds, and 2 control rounds) were prepped using the Direct RNA sequencing kit (Oxford Nanopore Technologies, #SQK-RNA002) with T4 DNA Ligase (NEB, #E6056), SuperScript III Reverse Transcriptase (Thermo Fisher Scientific, #1808004), and RNAClean XP beads (Agencourt, # A63987), loading reactions with up to 500 ng polyA-tailed RNA generated with Dynabeads® mRNA Purification Kit (ThermoFisher Scientific, #61006). The R9.4 MinION flowcells were loaded with each library prep and sequencing carried out using the MinION software on the MinIT device to keep up with base calling. The fasta files (PRJNA640661) that passed quality control, were concatenated and transferred for all samples to perform bioinformatics. The fast5 files (PRJNA640661) were transferred for all direct RNAseq datasets.

Quantification of each Nanopore fasta file was performed using minimap2[20] for quasi alignments to the Gencode.v31 transcriptome using nanopore settings (-ax splice -uf -k14) followed by quantification using Salmon_0.14.1[18]. All samples were merged together into a single file with transcript per million (TPM) data using the quantmerge function of Salmon followed by analysis with NetworkAnalysis[21] set to summing ensemble transcripts to gene annotation and significant genes determined using Limma[22] with padj <0.01 and log2 fold change >2 or <−2. Direct RNAseq analysis was done by converting the multi fast5 into single fast5 format using muti_to_single_fast5 tool followed by resquiggling the fast5 with Tombo[23] tools. Sample modification analysis was done using the Tombo detect_modification in model_sample_compare mode for comparison of control direct data relative to PCR amplified control fast5 files and level_sample_compare mode for control vs DPM treatment. The top 100 modified sites for each was exported into Meme[24] for motif generation and String[25] for protein networks and gene ontology enrichment.

Single Cell RNAseq and Bioinformatics

On the seventh day of DPM exposure, 2 control organoids and 2 DPM exposed organoids were made into single cell suspensions for single-cell RNAseq. Organoids were placed into individual microcentrifuge tubes and washed with 1mL of PBS. Organoids were then resupended in a 100 μL of LiberaseTM (0.03 μg in 1mL Basal 2 media) for 10min at 37C.

Samples were gently dispersed with a wide bore pipet tip and pelleted and washed twice with PBS. The cell pellets were resuspended in PBS, passed through a 40 μm cell filter, and dead cells removed with StemCell EasySep dead cell removal kit. Samples were pelleted and resuspended in PBS + 0.04% bovine serum albumin (BSA) and submitted to the Van Andel Research Institute Genomics Core for library preparation with the 10X Genomics kit and sequencing with Illumina HiSeq6000. The fastq files (PRJNA640661) were put through the Alevin[26] pipeline for demultiplexing of the samples and alignment to the transcriptome (gencode v.30). Seurat[27,28] was used for cell cluster analysis and integration of the two organoid conditions. The parameters used for creating of object in Seurat where the data a subset of the data is extracted, normalized and variable features identified, were subset = nFeature_RNA > 500, selection.method = “vst”, and nfeatures = 2000. For the integration analysis in Seurat that uses both the control sample and DPM samples the parameters used for the PCA analysis were npcs= 50, and for the UMAP clustering parameters were dims = 1:40. For differential cell expression between the DPM exposed cell cluster and the control cell cluster, the statistical parameters were log2FC threshold of 0.25 and at least 0.1 percent expression in the cell cluster.

Results

Ribosomal reduced RNAseq

Ribosomal reduced RNAseq quantifies expression of both coding and noncoding RNA in a tissue. Gene ontology analysis of the 12 organoids tested show that biological processes of the genes that are downregulated in response to DPM exposure (286 genes using a qval<0.05 and log2FD below - 0.25) were the majority are mechanisms of cell replication (Supplemental Fig. S1)..These processes include nucleosome assembly (4.22 GO enrichment score), kinetochore organization (8.20), DNA replication initiation (6.39), mitotic anaphase (3.92), G1/S transition of mitotic cell cycle (3.14), and cell division (2.56). Enrichment of genes that are upregulated after DPM exposure (308 genes with a qval<0.05 and log2FC above 0.25) indicatedbiological processes like hypothalamus cell migration (17.45), axon guidance (3.17), neuron development (2.88), and postsynapse assembly (6.43) are affected. The data indicates that DPM treatment of cerebral organoids manifests changes to the transcriptome that are further explored using more advanced RNAseq platforms like Nanopore RNAseq and single-cell RNAseq which will look into RNA base pair modifications and how individual cell populations are affected by DPM, respectively.

Nanopore RNAseq

While ribosomal reduced RNAseq allows for quantification of transcripts, Nanopore RNAseq can identify nucleotide substitutions and transcript variants in tissues. Nanopore RNAseq involves passing nucleic acids, either PCR amplified cDNA or the RNA itself for transcriptomics, through a protein channel using voltage to annotate the base detection. The platform has been used sparingly on transcriptomics of iPSC-based differentiations to this point due to novelty. We took different rounds of cerebral organoids that were from four different iPSC lines, stable gene knockdowns (*CHD8, GATAD2B, ASXL3, TSC2*), and various chemical exposure groups were run on Nanopore RNAseq (Fig. 2A). A total of 12 of the samples were PCR amplified Nanopore RNAseq and 4 were done as direct RNAseq. The

four different iPSC lines show the highest degree of separation based on principle component analysis for PCR amplified samples. All the treatment groups and stable shRNA knockdown lines performed on sample AICS-0011 closely cluster based on principal component analysis. The highest stratification of data within this dataset is found for direct vs PCR amplification. Stratifying genes based on PCR vs Direct for cerebral organoid datasets shows an enrichment in genes involved in RNA binding (Fig. 2B, AdjP of 0.004).

With the direct RNAseq data, we were able to assess RNA base pair modification using four strategies: direct vs PCR fast5 data comparisons (Fig. 2C), control analysis of 5mC modification (Fig. 2D), *de novo* analysis of control modifications (Fig. 2E), and modification comparisons between control and DPM treatment (Fig. 3). The PCR amplification of RNA results in the loss of all RNA modifications in classical RNAseq strategies. Through techniques such as cerebral organoids used here, it is possible to capture high concentrations of polyA RNA (500ng) opening the door to directly feed the RNA into protein pores such as Nanopore followed by the detection of subtle changes in the predicted voltage signal. Through the normalization of direct RNAseq fast5 datasets, which contains Nanopore called bases and all voltage signal, we show that our cerebral organoids contain many sites of predicted modifications (Fig. 2C). The most significant modification observed occurs at a cytosine (C) of the *B4GAT1* transcript, where one can observe a shift of the scaffolded voltage signal for the direct (red, Fig. 2C) vs the PCR amplified (gray, Fig. 2C) site. Compiling the top 100 predicted modified sites of RNA transcripts for the control direct vs PCR amplified reveals several enriched motifs without any significant enrichment of gene ontology of modified transcripts.

With knowledge that the direct RNAseq shows modified bases of RNA, several strategies can be used to detect modification sites. First, it is possible to use the Tombo tool predictions for voltage changes resulting from 5-methylcytosine (5mC) modifications to the RNA (Fig. 2D). In these cases, the subtle changes of voltage signals for C residues can be observed to shift in a predicted way from the expected voltage signal based on machine learning algorithms. Multiple C residues within a short region of the TTR gene in our cerebral organoids show a shift of the scaffolded voltage signals (red, Fig. 2D) vs the expected position of the C residue (gray, Fig. 2D). A very strong motif is identified from 89 out of the top 100 predicted 5mC sites of RNA consisting of a G**C**T sequence with the C predicted methylated, and 30 out of the 100 reads connected to translational initiation ontology with enrichment FDR of 4.25e-43 (Fig. 2D). In some cases, novel motifs and modifications can be identified by a *de novo* algorithm of the Tombo tools. In the case of our cerebral organoids we identify high probability modifications with little motif power but an enrichment of ribosome connected genes (Fig. 2E).

We have shown that DPM treated organoids have alterations to the RNA base pair modifications found in the control sample based on comparison of fast5 aligned voltage signals (Fig. 3). The most significant predicted modification occurs at a C of the *TMEM14B* gene (Fig. 3A) where a significant voltage density can be observed for the site (Fig. 3B). *TMEM14B* is a marker of outer radial glia cells[29] indicating these cells are impacted by DPM treatment, suggesting a need for scRNAseq as done below. The analysis of the top 100 modified sites in control vs DPM direct RNAseq points to a C base modification, likely 5mC

in 53 of the modified transcripts (Fig. 3C). Most surprising was the overlap of oxidoreductase and mitochondrial biology within the genes for the top 100 modified sites (Fig. 3D). From String PubMed enriched genes, DPM modifies transcripts in mitochondrial function and Rett Syndrome (Fig. 3D with FDR of 2.85e-5) [30], indicative of a potential neurological syndromic connection of RNA base modifications and DPM exposure in early brain development.

Single-cell (sc)RNAseq

The combination of reduced ribosomal RNAseq and nanopore sequencing exposes possible mechanisms of DPM in early brain development within a subset of cells that bulk data cannot resolve. The biological processes identified in ribosomal reduced RNAseq analyses show that mechanisms of cellular replication are downregulated in organoids exposed to DPM. The additional insight from Nanopore sequencing identified outer radial glia cells as a potential target of DPM. As the cerebral organoids are a 3-dimensional model of the brain, there are multiple distinct cell populations. Single-cell RNAseq was used to probe these distinct cell populations with the cerebral organoids and any affects that DPM exposure may have on these cellular populations or development over time.

Integration analysis of both the DPM exposed organoids and the control organoids using Seurat[27,28] shows 19 distinct clusters of cells (Fig. 4A). Identities of the cell clusters were determined using canonical cell markers and comparison to recent scRNAseq papers[31] as shown in Supplemental Table S1 and Figure S2–S4. The largest portion of subclustering was based on cell cycle genes contributing to G2/M phase (groups F, M, R; far right Supplemental Fig. S5), S phase (groups A, C, N; central Supplemental Fig. S5), and G1 phase (groups B, D, E, G, H, I, J, K, L, S; left outside, Supplemental Fig. S5). Further the separation can be defined around the presence or absence of SOX genes primarily *SOX2*, *SOX9*, and *SOX5* (Fig. S2), critical markers of neuronal progenitors and maturation. Radial glia can be separated into two groups, *SOX2* positive (B, C, N, M) and *SOX2*/*SOX9* positive (A, F, G), each clustering with separation of cell cycle. Coming off of the *SOX2*/*SOX9* positive G1 radial glia is also a clustering of cells (group L) that show a unique list of enriched genes involved in stress response (Supplemental Fig. S6) that indicate hypoxia induced damage of cerebral organoid maturation.

According to pseudo time analysis (Supplemental Fig. S7) of the cell clusters, group A S-phase radial glia cells that are *SOX2*/*SOX9* positive give rise to cell groups K, E, H, and O. Each of these groups has the expression of *SOX2* and absence of *SOX9*. Group H are *SOX2*/*SOX9* developing neurons that express multiple markers of mature neurons (*MAP2*, *MAPT*). The group O cell cluster still transcribe *SOX2* but also express *EOMES* and *ASCL1*, markers of intermediate progenitors. Group K has very few genes that distinguish identify and remains unknown without *SOX2* or *SOX9,* suggesting a maturing neuron identity. The Group E cells derive from the group K and have no *SOX2*/*SOX9* with additional expression of maturing neurons including *NEFL*, *MAPT*, *NRN1*, *VAMP2*, *STMN3*, and *STXBP1*. Coming off group E is then group D that has the expression of *SOX5* along with glutamatergic neuron markers *GRIN2B*, *SLC17A7*, *NEUROD6*, *GRIA2*, *GRIA1*, *DLG4*, *GAP43*, *SYP*. Also arising out of the group E cluster is group J, which have expression of

genes suggestive of immature neurons (*MAP2, RBFOX3, SYP, DCX, NEUROD1, TBR1, TUBB3, STMN1*).

Two groups of cells are uniquely outliers from the rest of the clustering, S and P. Group P cells are annotated as Mesenchymal/Neural Crest cells with expression of epithelial-to-mesenchymal genes (*COL3A1, DCN, COL1A2, FN1, SNAI2, VIM*) critical for neural migration. Group S cells are fewer in number and suggested to be choroid plexus-like based on the expression of *TTR, PIFO, OTX2*. Deriving from the group G G1 radial glia is the group I cells identified as G1 Outer Radial Glia that have expression of both *SOX2* and *SOX9* with additional expression of genes *HOPX* and *FAM107A* that are known markers of the group.

The integration analysis shows that certain cell groups have noticeable differences in the populations between the control organoids and the DPM exposed organoids. A log2 fold enrichment shows that the group of outer radial glia cells are 1.75 more enriched in the control organoid cell density when compared with the DPM organoids (Fig. 4B). This aligns with our nanopore sequencing data that also showed modification differences of *TMEM14B,* a marker for outer radial glia. In humans, outer radial glia are located in the outer subventricular zone and produce deep and upper cortical layer neurons[32].

Differential gene expression analysis of each cell cluster between the control and DPM organoids were performed on all clusters except for G2/M-phase immature neurons and choroid plexus clusters as they do not contain any DPM exposed cells (Supplemental Table S1). A closer examination of the downregulated genes due to DPM exposure shows a pattern of metabolic processes being affected. The biological processes include oxidative phosphorylation (11 cell clusters), aerobic respiration (10), cellular respiration (10), electron transport coupled proton transport (10), ATP synthesis coupled electron transport (11), and mitochondrial respiratory chain complex I assembly (7). Inhibition of Complex I of OXPHOS causes increases in reactive oxygen species like superoxide[33,34]. When comparing the fold enrichment of oxidative phosphorylation with mitochondrial respiratory chain complex I assembly and aerobic respiration, the enrichment of oxidative phosphorylation in each cell cluster is more commonly larger than the other to biological processes (Supplemental Fig. S8A). A closer analysis of the downregulated genes that map to oxidative phosphorylation revealed that many also are genes that make up Complex I of oxidative phosphorylation (Supplemental Fig. S8B). The clusters with reduced oxidative phosphorylation processes are diverse, including both radial glia and neurons, the majority of which express markers for G1 cell cycle phase. Inhibition of oxidative phosphorylation in neural stem cells has been shown to decrease proliferation and can cause cells to remain in the G1/S phase longer than normal, ultimately affecting neuronal diversity[35]. Postmortem brain samples of autistic individuals show reduced neuron density in cortical regions of the brain[36].This enrichment of downregulated OxPHOS genes indicates that DPM exposure during development may affect the cells ability to proliferate into other cells types.

In addition, there is overlap between cell groups involved in oxidative phosphorylation and biological processes involved in processing oxidative stress, cellular stress (Supplemental Fig. S8C). Comparing all the genes in the 11 cell clusters that map to oxidative

phosphorylation with all the genes in the 6 groups involved in response to oxidative stress, there are only 7 genes that overlap between the two gene lists. A closer look at outer radial glia cells show that there is some overlap in the genes involved in response to oxidative stress and oxidative phosphorylation. This data indicates that DPM is affecting both oxidative stress and oxidative phosphorylation pathways.

Integrating differential expression among clusters, we identify multiple groups with similar genes (Fig. 4C). The top 10 genes include *TTR, NMNAT3, WDPCP, MIPOL1, CFAP54, REL, KPNA5, TBC1D8B, PTPRZ1, PCDH11Y* (red Fig. 4C, Supplemental Fig. S9), all of which have differential expression in at least 7 cell clusters. *TTR* is seen differentially expressed in 14 different cell groups. Further interrogation for the number of genes differentially expressed in each of the cell groups shows a high number of differential genes in groups J, A, L, and I (Fig. 4D). From at least three of these four groups there are 97 genes overlapping DPM changes, with a significant KEGG enrichment of disease biology (Parkinson's and Huntington's) and oxidative phosphorylation (Fig. 4E). Outer radial glia cells (group I) are the origin of most deep layer cortical neurons and the cell group affected the most DPM exposure. DPM impact on outer radial glia differentiation could explain how environmental pollutants like DPM can cause neurodevelopmental disorders like ASD by preventing differentiation of earlier cell populations like the outer radial glia from forming the mature neurons that populate deeper layers of the cortex.

Expression of the Simons Foundation Autism Research Initiative (SFARI)[37] genes linked to ASD, specifically the category 1 genes with "high confidence", shows that expression of theses known ASD associated genes are variable across the cell groups identified in the single cell analysis (Supplemental Fig. S10). Some of these cell groups consist of cells that have less than 25 percent of the cells expressing the SFARI category 1 genes. Groups such as L, J, I, H, F, and D show marked elevation of both the number of cells expressing the gene but also have an elevated expression of these ASD risk genes. Integration of all SFARI category 1–3 and syndromic annotated genes with our cell group differential expression identifies 34 genes impacted by DPM (cyan, Fig. 4C) with 1 gene (*AGO3*) with differential expression in 6 different clusters, one gene in five cluster (*TBCK*), two genes in 4 clusters (*MYT1L, SLC6A4*), two genes in 3 clusters (*UBN2, PRKN*), and three genes in 2 clusters (*CHD1, DIP2A, DYNC1H1*). From the group J, A, L, and I with high levels of differential gene expression, we also observe high levels of ASD genes impacted by DPM (Fig. 4D). Overall, our data suggests that DPM can impact oxidative phosphorylation and expression of genes previously implicated in ASD in a subset of cerebral organoid cell clusters.

Discussion/Conclusion

The field of toxicogenomics looks to understand the genetic responses to toxicants and environmental substances[38]. While animal models are commonly used for toxicogenomic experiments, it has been widely shown in the drug discovery field that animal models can fail to predict or recapitulate toxicity in humans. In contrast, human toxicology is limited by the inability to directly study molecular mechanisms in humans, due to a sparsity of samples and the inability to test compounds on diverse physiological environments of multicellular organs which are not captured in typical cell culture systems. This paradox requires a unique

solution to probing the field of toxicogenomics in humans. In addition, many toxicogenomic studies utilize either bulk tissue RNAseq, which looks at the full transcript but requires short reads, or microarray platforms which only profiles a subset of genes/transcripts. To examine how toxicants ultimately affect human prenatal brain development, we found that using cerebral organoids is a promising avenue of research owing to the diversity of cell types, recapitulation of relevant molecular developmental processes, and the experimental control of the environment. Our use of multiple sequencing technologies allows for a more robust insight into how DPM effects early brain development by not only being able to compare our organoid data with other transcriptomic experiments on DPM exposure but also utilizes newer sequencing technologies like single-cell and nanopore sequencing to look at both changes to distinct cell populations and posttranscriptional modifications to the RNA itself. While the approach presented here is innovative by combining multiple sequencing platforms, it is important to highlight that each technique gives unique and different information. The ribosomal reduced RNAseq and nanopore sequencing give information for the bulk organoid as a whole whereas single cell RNAseq is sequencing individual cells. Single-cell RNAseq is known to have limitations of low capture efficiency, high dropout rates, and data that is noisier and more variable than traditional sequencing.[39] Data analysis techniques are still improving base pair calling in Nanopore sequencing.[40] The three techniques can be integrated to provide a more robust understanding of exposures responses.

The use of this multi-sequencing approaches using human cerebral organoids show how each technique brings a different insight to the transcriptional changes that occur during DPM exposure, with a remarkable overlap of cell types and biological pathways. Our combinatorial approach shows that basic cellular processes involved in cell proliferation and metabolism are affected by DPM exposure in developing human cerebral cortex. Our finding that oxidative phosphorylation is the biological process most widely affected by DPM could indicate that early dysfunction of metabolism prevents normal cell differentiation and function in the developing brains. Such *in utero* insults and their lasting impacts on neuronal lineages and dependent circuits may therefore contribute to the environmental component of the etiology of neurodevelopmental disorders. This insight into the effect of DPM on neurodevelopmental disorders is an important follow up to previous epidemiological studies that correlate prenatal DPM exposure to neurodevelopmental disorders. Evidence of this correlation between prenatal exposure and neurodevelopmental disorders is limited, but other studies in rodent models have tied prenatal particulate matter exposure to inflammatory responses in mouse pups [41], downregulation of mitochondrial function genes [42], and immune responses [43].The data presented here shows that DPM exposure fundamentally affects normal cellular functions. The single-cell RNAseq builds on the data from reduced ribosomal RNAseq that shows mechanisms of cell division are downregulated by indicating the initial impact on cells seems to occur to the mitochondria. Our data indicates that DPM is affecting normal cell metabolism through dysfunction in oxidative phosphorylation and downregulation of the complexes of the electron transport chain.

Mitochondria are important organelles that play a diverse role in cellular biology. Oxidative phosphorylation is the process in the mitochondria where ATP is generated via the electron transport chain. This generation of ATP in the brain is extremely important for the energy

production of ATP in neurons but also for its role in neuronal plasticity[44], neurogenesis[45], and synaptogenesis[46]. This pool of mitochondrial produced ATP is utilized for brain cell functions including axon growth[47] and synaptic transmission[48]. Given the important role of OXPHOS generation of ATP in brain development, it is perhaps not surprising that mitochondrial dysfunction, oxidative stress, and disordered OxPHOS pathways and oxidative stress has been linked to neurodevelopmental disorders like epilepsy[49] and intellectual disabilities like ASD[50], Rett syndrome[51], fragile X[52] and down syndrome[53].

Many transcriptional studies have also noted a downregulation of genes in the electron transport chain by looking at RNAseq data from different brain regions in postmortem ASD brains[54] and microarray data of the cerebral cortex[55]. In addition to transcriptional downregulation, reduced concentrations of ETC complex proteins were also found in ASD brains[56]. Copy number variants of autistic patients are commonly found in genes integral to oxidative phosphorylation.[57] OxPHOS defects also disrupt cortical interneuron migration, a key step in brain development, and caused interneurons to lose polarity.[58] Abnormalities of mitochondria were found in patients with Rett syndrome, a syndromic form of ASD caused by mutations in *MECP2*[51,59]. Rett syndrome patients have impaired mitochondria and redox function[60], mitochondrial genes are differentially expressed in Rett patients[61], with reduced ATP concentrations[62]. Our data expands on these observations found through a combination of patient samples, animal models, and traditional 2-D cellular cultures by using 3-D cerebral organoids in conjunction with traditional transcriptional studies, with single-cell RNAseq, and Nanopore sequencing to examine RNA base modifications, to examine how early environmental exposure can exacerbate genetically predisposed intellectual disabilities.

RNA base modifications amount to over 100 different types with the field just beginning to map transcriptome wide modifications, with little insights into the dynamic processes that occur due to environmental changes. Previous studies looking at base modifications of RNA have been limited to single targets with advanced biochemical assays or multistep chemical conversions followed by sequencing.[63] From these early high impact studies it is known that the epitranscriptome modifications range from N6-methyladenosine (m6A), 5-methylcytosine (m5C), to pseudouridine that can impact all forms of RNA[64] through all steps of RNA life cycles[65] including mRNA enhanced translation[66] and RNA interaction with translation machinery[67].

The development of Nanopore based chemistry, where RNA molecules pass across a protein pore and yield a voltage signal, has allowed for the analysis of subtle changes in voltage signal relative to the predicted voltage of a base. This enables for a transcriptome wide analysis of an exposure group like DPM on RNA modifications, a significant development in the field of toxicogenomics. We show here one of the first environmental exposure studies on iPSC based cerebral organoids, identifying dynamic RNA modifications in response to exposure. The need for high amounts of RNA to perform these analyses in Nanopore chemistry limits the utility of these techniques to human primary samples. However, development of cerebral organoids, where a hundred organoids can be treated and pooled,

allows us a unique ability to assess consensus direct RNA modifications on human model systems, a potentially groundbreaking platform for toxicogenomics moving forward.

In our current work we show that cerebral organoids contain modified RNA and further show that the RNA modifications reflect DPM associated changes. One of the most interesting observations is that *TTR* is predicted to be the most statistically methylated transcripts in the cerebral organoids (Fig. 2D) and is also the most consistently downregulated transcripts in cerebral organoids treated with DPM in 14 different cell clusters (Fig. 4C). Further work is needed to understand if this observation is mechanistic. *TTR* codes for the Transthyretin protein, known to be involved in nerve cell glycolysis, nerve cell regeneration, and axon growth[68–70]. In disorders such as Alzheimer's disease the protein has been suggested to inhibit toxicity of protein misfolding[71]. Several endocrine disrupting chemicals such as BPA have also been shown to impact RNA levels of Transthyretin[72]. Transthyretin has also been connected to changes in proteomics of ASD patients[73]. While DNA modifications such as methylation have been shown to correlate with ASD development[74], few labs have addressed the role of RNA modifications transcriptome wide in neuron development or in disease states. Adenosine-to-inosine modifications have been suggested to impact synaptic genes impacting risk of autism[75] and many modifications have been suggested to alter the nervous system[76]. Our connection of DPM exposure modified genes involved in mitochondrial function to those altered in ASD linked Rett syndrome builds a strong connection of RNA modifications impacting metabolic processes within the developing cerebral organoid. The further connection of RNA modifications to the cell types and biological processes identified in our single cell RNAseq suggest that DPM exposure to the cerebral organoids would serve as a risk factor for ASD like development.

We have presented here the integration of a multi-transcriptomic approach to examine the mechanisms of prenatal DPM exposure that epidemiological studies have correlated to neurodevelopmental disorders. By utilizing this 3-pronged approach we attempted to overcome the limitations of each individual technique. Each technique is compelmentary by showing that the genes *TTR* is shown to be downregulated in several cell clusters in the single cell data but the RNA has a posttranscriptional modification to incorporated a methylation when exposed to DPM. This integrated approach highlights a way to study the effects of toxicants on both posttranscriptional modifications and the effects to specific cell populations.

Supplementary Material

Refer to Web version on PubMed Central for supplementary material.

Acknowledgement

The authors thank the Van Andel Institute Genomics Core for providing facilities and RNA sequencing services

Funding Sources

This work was funded by NIH R56ES029064 (to DBC), NIH K01ES025435 (to JWP), the Spectrum-MSU Alliance Fund, and Michigan State University.

Statement of Ethics

This study has been granted an exemption from requiring ethics approval because all iPSC lines were deidentified and from repositories.

References

1. Wells JCK. The thrifty phenotype as an adaptive maternal effect. Biological Reviews. 2007;82(1):143–72. [PubMed: 17313527]
2. Skogen JC, Øverland S. The fetal origins of adult disease: a narrative review of the epidemiological literature. JRSM Short Rep. 2012 8;3(8). DOI: 10.1258/shorts.2012.012048
3. Gluckman PD, Hanson MA, Cooper C, Thornburg KL. Effect of in utero and early-life conditions on adult health and disease. N Engl J Med. 2008 7;359(1):61–73. [PubMed: 18596274]
4. Moody EC, Cantoral A, Tamayo-Ortiz M, Pizano-Zárate MaL, Schnaas L, Kloog I, et al. Association of Prenatal and Perinatal Exposures to Particulate Matter With Changes in Hemoglobin A1c Levels in Children Aged 4 to 6 Years. JAMA Netw Open. 2019 12;2(12). DOI: 10.1001/jamanetworkopen.2019.17643
5. Bell ML, Belanger K, Ebisu K, Gent JF, Lee HJ, Koutrakis P, et al. Prenatal Exposure to Fine Particulate Matter and Birth Weight. Epidemiology. 2010 11;21(6):884–91. [PubMed: 20811286]
6. Volk HE, Lurmann F, Penfold B, Hertz-Picciotto I, McConnell R. Traffic-Related Air Pollution, Particulate Matter, and Autism. JAMA Psychiatry. 2013 1;70(1):71–7. [PubMed: 23404082]
7. Lanphear Bruce P., Hornung Richard, Khoury Jane, Yolton Kimberly, Baghurst Peter, Bellinger David C, et al. Low-Level Environmental Lead Exposure and Children's Intellectual Function: An International Pooled Analysis. Environmental Health Perspectives. 2005 7;113(7):894–9. [PubMed: 16002379]
8. Guerri C. Mechanisms involved in central nervous system dysfunctions induced by prenatal ethanol exposure. neurotox res. 2002 1;4(4):327–35. [PubMed: 12829422]
9. Jedrychowski WA, Perera FP, Camann D, Spengler J, Butscher M, Mroz E, et al. Prenatal exposure to polycyclic aromatic hydrocarbons and cognitive dysfunction in children. Environ Sci Pollut Res. 2015 3;22(5):3631–9.
10. Chen Aimin, Kimberly Yolton, Rauch Stephen A., Webster Glenys M., Hornung Richard, Sjödin Andreas, et al. Prenatal Polybrominated Diphenyl Ether Exposures and Neurodevelopment in U.S. Children through 5 Years of Age: The HOME Study. Environmental Health Perspectives. 2014 8;122(8):856–62. [PubMed: 24870060]
11. Lui JH, Hansen DV, Kriegstein AR. Development and evolution of the human neocortex. Cell. 2011 7;146(1):18–36. [PubMed: 21729779]
12. Smart IHM, Dehay C, Giroud P, Berland M, Kennedy H. Unique morphological features of the proliferative zones and postmitotic compartments of the neural epithelium giving rise to striate and extrastriate cortex in the monkey. Cereb Cortex. 2002 1;12(1):37–53. [PubMed: 11734531]
13. Hecht PM, Ballesteros-Yanez I, Grepo N, Knowles JA, Campbell DB. Noncoding RNA in the transcriptional landscape of human neural progenitor cell differentiation. Front Neurosci. 2015;9:392. [PubMed: 26557050]
14. La Manno G, Gyllborg D, Codeluppi S, Nishimura K, Salto C, Zeisel A, et al. Molecular Diversity of Midbrain Development in Mouse, Human, and Stem Cells. Cell. 2016 10;167(2):566-580.e19.
15. Hodge RD, Bakken TE, Miller JA, Smith KA, Barkan ER, Graybuck LT, et al. Conserved cell types with divergent features in human versus mouse cortex. Nature. 2019 9;573(7772):61–8. [PubMed: 31435019]
16. Lancaster MA, Renner M, Martin C-A, Wenzel D, Bicknell LS, Hurles ME, et al. Cerebral organoids model human brain development and microcephaly. Nature. 2013 9;501(7467):373–9. [PubMed: 23995685]
17. Liu Z, Huang R, Roberts R, Tong W. Toxicogenomics: A 2020 Vision. Trends Pharmacol Sci. 2019;40(2):92–103. [PubMed: 30594306]
18. Patro R, Duggal G, Love MI, Irizarry RA, Kingsford C. Salmon provides fast and bias-aware quantification of transcript expression. Nat Methods. 2017 4;14(4):417–9. [PubMed: 28263959]

19. Love MI, Huber W, Anders S. Moderated estimation of fold change and dispersion for RNA-seq data with DESeq2. Genome Biology. 2014 12;15(12):550. [PubMed: 25516281]
20. Li H. Minimap2: pairwise alignment for nucleotide sequences. Bioinformatics. 2018 15;34(18):3094–100. [PubMed: 29750242]
21. Zhou G, Soufan O, Ewald J, Hancock REW, Basu N, Xia J. NetworkAnalyst 3.0: a visual analytics platform for comprehensive gene expression profiling and meta-analysis. Nucleic Acids Res. 2019 4 DOI: 10.1093/nar/gkz240
22. Ritchie ME, Phipson B, Wu D, Hu Y, Law CW, Shi W, et al. limma powers differential expression analyses for RNA-sequencing and microarray studies. Nucleic Acids Res. 2015 4;43(7):e47.
23. Stoiber M, Quick J, Egan R, Lee JE, Celniker S, Neely RK, et al. De novo Identification of DNA Modifications Enabled by Genome-Guided Nanopore Signal Processing. bioRxiv. 2017 4;094672.
24. Machanick P, Bailey TL. MEME-ChIP: motif analysis of large DNA datasets. Bioinformatics. 2011 6;27(12):1696–7. [PubMed: 21486936]
25. Franceschini A, Szklarczyk D, Frankild S, Kuhn M, Simonovic M, Roth A, et al. STRING v9.1: protein-protein interaction networks, with increased coverage and integration. Nucleic Acids Res. 2013 1;41(Database issue):D808–815. [PubMed: 23203871]
26. Srivastava A, Malik L, Smith T, Sudbery I, Patro R. Alevin efficiently estimates accurate gene abundances from dscRNA-seq data. Genome Biology. 2019 3;20(1):65. [PubMed: 30917859]
27. Butler A, Hoffman P, Smibert P, Papalexi E, Satija R. Integrating single-cell transcriptomic data across different conditions, technologies, and species. Nature Biotechnology. 2018 5;36(5):411–20.
28. Stuart T, Butler A, Hoffman P, Hafemeister C, Papalexi E, Mauck WM, et al. Comprehensive Integration of Single-Cell Data. Cell. 2019 6;177(7):1888-1902.e21.
29. Liu J, Liu W, Yang L, Wu Q, Zhang H, Fang A, et al. The Primate-Specific Gene TMEM14B Marks Outer Radial Glia Cells and Promotes Cortical Expansion and Folding. Cell Stem Cell. 2017 11;21(5):635-649.e8.
30. Pecorelli A, Leoni G, Cervellati F, Canali R, Signorini C, Leoncini S, et al. Genes related to mitochondrial functions, protein degradation, and chromatin folding are differentially expressed in lymphomonocytes of Rett syndrome patients. Mediators Inflamm. 2013;2013:137629.
31. Kanton S, Boyle MJ, He Z, Santel M, Weigert A, Sanchís-Calleja F, et al. Organoid single-cell genomic atlas uncovers human-specific features of brain development. Nature. 2019 10;574(7778):418–22. [PubMed: 31619793]
32. Pollen AA, Nowakowski TJ, Chen J, Retallack H, Sandoval-Espinosa C, Nicholas CR, et al. Molecular Identity of Human Outer Radial Glia During Cortical Development. Cell. 2015 9;163(1):55–67. [PubMed: 26406371]
33. Raha S, Robinson BH. Mitochondria, oxygen free radicals, disease and ageing. Trends in Biochemical Sciences. 2000 10;25(10):502–8. [PubMed: 11050436]
34. Kussmaul L, Hirst J. The mechanism of superoxide production by NADH:ubiquinone oxidoreductase (complex I) from bovine heart mitochondria. PNAS. 2006 5;103(20):7607–12. [PubMed: 16682634]
35. van den Ameele J, Brand AH. Neural stem cell temporal patterning and brain tumour growth rely on oxidative phosphorylation. eLife. 8. DOI: 10.7554/eLife.47887
36. van Kooten IAJ, Palmen SJMC, von Cappeln P, Steinbusch HWM, Korr H, Heinsen H, et al. Neurons in the fusiform gyrus are fewer and smaller in autism. Brain. 2008 4;131(Pt 4):987–99. [PubMed: 18332073]
37. Abrahams BS, Arking DE, Campbell DB, Mefford HC, Morrow EM, Weiss LA, et al. SFARI Gene 2.0: a community-driven knowledgebase for the autism spectrum disorders (ASDs). Mol Autism. 2013 10;4(1):36. [PubMed: 24090431]
38. Waters MD, Fostel JM. Toxicogenomics and systems toxicology: aims and prospects. Nature Reviews Genetics. 2004 12;5(12):936–48.
39. Chen G, Ning B, Shi T. Single-Cell RNA-Seq Technologies and Related Computational Data Analysis. Front Genet. 2019;10. DOI: 10.3389/fgene.2019.00317

40. Rang FJ, Kloosterman WP, de Ridder J. From squiggle to basepair: computational approaches for improving nanopore sequencing read accuracy. Genome Biol. 2018 7;19. DOI: 10.1186/s13059-018-1462-9
41. Klocke C, Sherina V, Graham UM, Gunderson J, Allen JL, Sobolewski M, et al. Enhanced cerebellar myelination with concomitant iron elevation and ultrastructural irregularities following prenatal exposure to ambient particulate matter in the mouse. Inhal Toxicol. 2018;30(9–10):381–96. [PubMed: 30572762]
42. Guo Y, Cao Z, Jiao X, Bai D, Zhang Y, Hua J, et al. Pre-pregnancy exposure to fine particulate matter (PM2.5) increases reactive oxygen species production in oocytes and decrease litter size and weight in mice. Environ Pollut. 2020 10;115858.
43. Haghani A, Johnson R, Safi N, Zhang H, Thorwald M, Mousavi A, et al. Toxicity of urban air pollution particulate matter in developing and adult mouse brain: Comparison of total and filter-eluted nanoparticles. Environment International. 2020 3;136:105510.
44. Mattson MP. Mitochondrial Regulation of Neuronal Plasticity. Neurochem Res. 2007 4;32(4):707–15. [PubMed: 17024568]
45. Xavier JM, Rodrigues CMP, Solá S. Mitochondria: Major Regulators of Neural Development. Neuroscientist. 2016;22(4):346–58. [PubMed: 25948649]
46. Lee CW, Peng HB. The Function of Mitochondria in Presynaptic Development at the Neuromuscular Junction. Mol Biol Cell. 2008 1;19(1):150–8. [PubMed: 17942598]
47. Vaarmann A, Mandel M, Zeb A, Wareski P, Liiv J, Kuum M, et al. Mitochondrial biogenesis is required for axonal growth. Development. 2016 6;143(11):1981–92. [PubMed: 27122166]
48. Evans RJ, Derkach V, Surprenant A. ATP mediates fast synaptic transmission in mammalian neurons. Nature. 1992 6;357(6378):503–5. [PubMed: 1351659]
49. Folbergrová J, Kunz WS. Mitochondrial dysfunction in epilepsy. Mitochondrion. 2012 1;12(1):35–40. [PubMed: 21530687]
50. Valiente-Pallejà A, Torrell H, Muntané G, Cortés MJ, Martínez-Leal R, Abasolo N, et al. Genetic and clinical evidence of mitochondrial dysfunction in autism spectrum disorder and intellectual disability. Hum Mol Genet. 2018 3;27(5):891–900. [PubMed: 29340697]
51. Cornford ME, Philippart M, Jacobs B, Scheibel AB, Vinters HV. Neuropathology of Rett Syndrome: Case Report With Neuronal and Mitochondrial Abnormalities in the Brain. J Child Neurol. 1994 10;9(4):424–31. [PubMed: 7822737]
52. Bechara EG, Didiot MC, Melko M, Davidovic L, Bensaid M, Martin P, et al. A Novel Function for Fragile X Mental Retardation Protein in Translational Activation. PLoS Biol. 2009 1;7(1). DOI: 10.1371/journal.pbio.1000016
53. Helguera P, Seiglie J, Rodriguez J, Hanna M, Helguera G, Busciglio J. Adaptive Downregulation of Mitochondrial Function in Down Syndrome. Cell Metabolism. 2013 1;17(1):132–40. [PubMed: 23312288]
54. Ginsberg MR, Rubin RA, Falcone T, Ting AH, Natowicz MR. Brain Transcriptional and Epigenetic Associations with Autism. PLOS ONE. 2012 9;7(9):e44736.
55. Schwede M, Nagpal S, Gandal MJ, Parikshak NN, Mirnics K, Geschwind DH, et al. Strong correlation of downregulated genes related to synaptic transmission and mitochondria in postmortem autism cerebral cortex. Journal of Neurodevelopmental Disorders. 2018 6;10(1):18. [PubMed: 29859039]
56. Chauhan A, Gu F, Essa MM, Wegiel J, Kaur K, Brown WT, et al. Brain region-specific deficit in mitochondrial electron transport chain complexes in children with autism. Journal of Neurochemistry. 2011;117(2):209–20. [PubMed: 21250997]
57. Smith M, Flodman PL, Gargus JJ, Simon MT, Verrell K, Haas R, et al. Mitochondrial and Ion Channel Gene Alterations in Autism. Biochim Biophys Acta. 2012 10;1817(10):1796–802. [PubMed: 22538295]
58. Lin-Hendel EG, McManus MJ, Wallace DC, Anderson SA, Golden JA. Differential Mitochondrial Requirements for Radially and Non-radially Migrating Cortical Neurons: Implications for Mitochondrial Disorders. Cell Reports. 2016 4;15(2):229–37. [PubMed: 27050514]

59. Dotti MT, Manneschi L, Malandrini A, De Stefano N, Caznerale F, Federico A. Mitochondrial dysfunction in Rett syndrome: An ultrastructural and biochemical study. Brain and Development. 1993 3;15(2):103–6. [PubMed: 8214327]
60. Großer E, Hirt U, Janc OA, Menzfeld C, Fischer M, Kempkes B, et al. Oxidative burden and mitochondrial dysfunction in a mouse model of Rett syndrome. Neurobiology of Disease. 2012 10;48(1):102–14. [PubMed: 22750529]
61. Pecorelli A, Leoni G, Cervellati F, Canali R, Signorini C, Leoncini S, et al. Genes Related to Mitochondrial Functions, Protein Degradation, and Chromatin Folding Are Differentially Expressed in Lymphomonocytes of Rett Syndrome Patients [Internet]. Mediators of Inflammation. 2013;2013:e137629.
62. Saywell V, Viola A, Confort-Gouny S, Le Fur Y, Villard L, Cozzone PJ. Brain magnetic resonance study of Mecp2 deletion effects on anatomy and metabolism. Biochemical and Biophysical Research Communications. 2006 2;340(3):776–83. [PubMed: 16380085]
63. Li X, Xiong X, Yi C. Epitranscriptome sequencing technologies: decoding RNA modifications. Nat Methods. 2016 29;14(1):23–31. [PubMed: 28032622]
64. Li S, Mason CE. The pivotal regulatory landscape of RNA modifications. Annu Rev Genomics Hum Genet. 2014;15:127–50. [PubMed: 24898039]
65. Roundtree IA, Evans ME, Pan T, He C. Dynamic RNA Modifications in Gene Expression Regulation. Cell. 2017 6;169(7):1187–200. [PubMed: 28622506]
66. Gilbert WV, Bell TA, Schaening C. Messenger RNA modifications: Form, distribution, and function. Science. 2016 6;352(6292):1408–12. [PubMed: 27313037]
67. Wang X, Zhao BS, Roundtree IA, Lu Z, Han D, Ma H, et al. N(6)-methyladenosine Modulates Messenger RNA Translation Efficiency. Cell. 2015 6;161(6):1388–99. [PubMed: 26046440]
68. Vieira M, Saraiva MJ. Transthyretin: a multifaceted protein. Biomol Concepts. 2014 Mar;5(1):45–54.
69. Fleming CE, Saraiva MJ, Sousa MM. Transthyretin enhances nerve regeneration. J Neurochem. 2007 10;103(2):831–9. [PubMed: 17897357]
70. Zawiślak A, Jakimowicz P, McCubrey JA, Rakus D. Neuron-derived transthyretin modulates astrocytic glycolysis in hormone-independent manner. Oncotarget. 2017 12;8(63):106625–38.
71. Giunta S, Valli MB, Galeazzi R, Fattoretti P, Corder EH, Galeazzi L. Transthyretin inhibition of amyloid beta aggregation and toxicity. Clin Biochem. 2005 12;38(12):1112–9. [PubMed: 16183049]
72. Singh S, Li SS-L. Bisphenol A and phthalates exhibit similar toxicogenomics and health effects. Gene. 2012 2;494(1):85–91. [PubMed: 22173104]
73. Ngounou Wetie AG, Wormwood K, Thome J, Dudley E, Taurines R, Gerlach M, et al. A pilot proteomic study of protein markers in autism spectrum disorder. Electrophoresis. 2014 7;35(14):2046–54. [PubMed: 24687421]
74. Ladd-Acosta C, Hansen KD, Briem E, Fallin MD, Kaufmann WE, Feinberg AP. Common DNA methylation alterations in multiple brain regions in autism. Mol Psychiatry. 2014 8;19(8):862–71. [PubMed: 23999529]
75. Eran A, Li JB, Vatalaro K, McCarthy J, Rahimov F, Collins C, et al. Comparative RNA editing in autistic and neurotypical cerebella. Mol Psychiatry. 2013 9;18(9):1041–8. [PubMed: 22869036]
76. Satterlee JS, Basanta-Sanchez M, Blanco S, Li JB, Meyer K, Pollock J, et al. Novel RNA modifications in the nervous system: form and function. J Neurosci. 2014 11;34(46):15170–7.

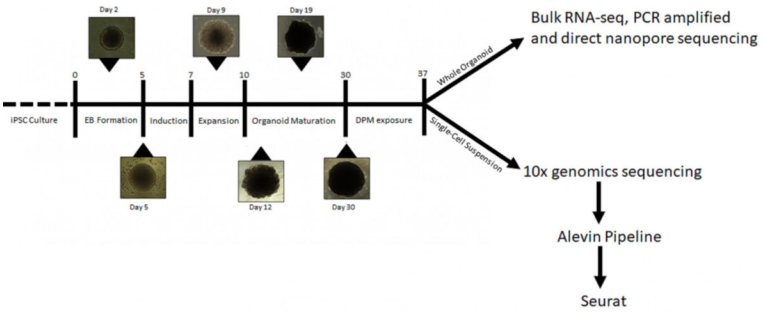

Fig. 1.

Overview of environmental exposure experiment with cerebral organoids. Cerebral organoids are matured to day 30 and then exposed to DPM for 7 days. These can then be analyzed using different sequencing technologies to probe the effects of DPM.

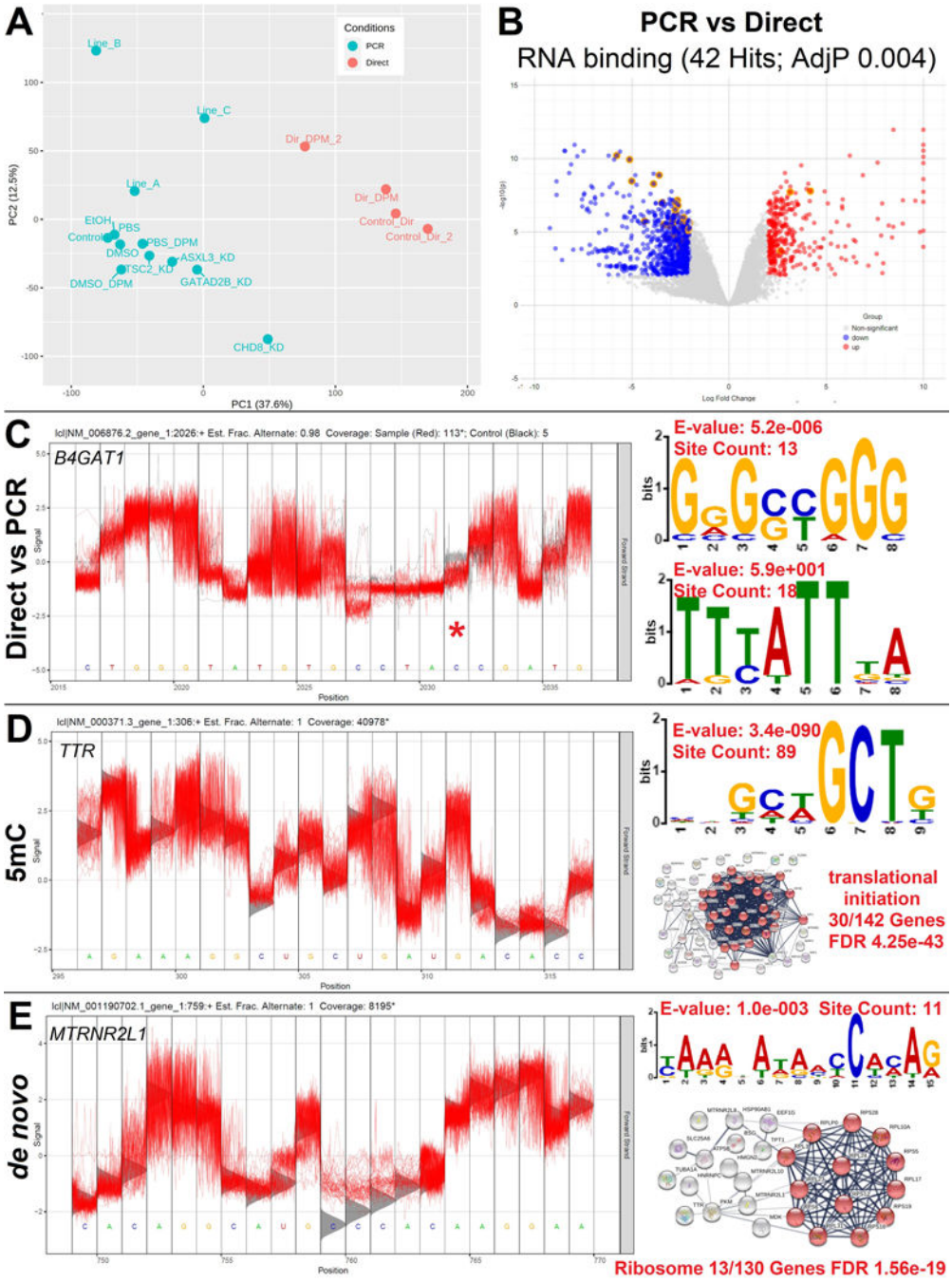

Fig. 2.

Nanopore PCR-amplified vs. Direct RNAseq. A) Principle component analysis of cerebral organoid samples for Nanopore PCR (cyan) or Direct (red) RNAseq. B) Volcano plot for genes significantly differentially expressed in PCR vs Direct RNAseq with RNA binding associated genes highlighted. C-E) Details for most significant modification of control Direct RNAseq using comparison to PCR amplified data (C), 5mC model prediction (D), and *de novo* predictions (E). Shown on the left of each is the voltage overlap of control reads (red) relative to PCR or expected positions (gray) for the most significant site detected. On

the right is the meme motif from the top 100 significant with statistics shown, and below that a String network with enriched ontology terms. The panel C does not have any significant enriched protein networks so shown is the second predicted motif.

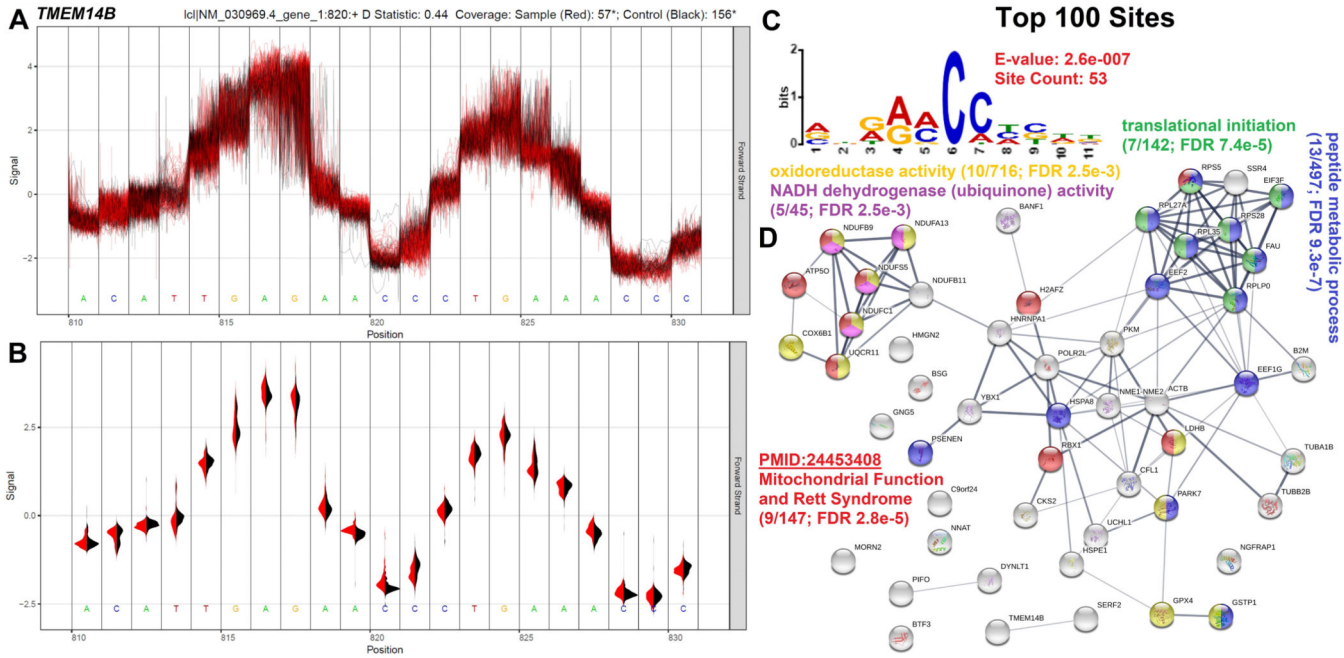

Fig. 3.

Control vs. DPM treatment using Nanopore Direct RNAseq. A) Voltage overlay for the top predicted modification found in the *TMEM14B* gene. DPM treatment reads are in red and control in black. B) Density plot for the voltage signal in panel A with DPM in red and control in black. C) Meme motif prediction from the top 100 predicted modified sites between control and DPM treatment. D) String network of genes found in the top 100 modified sites between control and DPM. Colors corresponded to the labeled enriched terms.

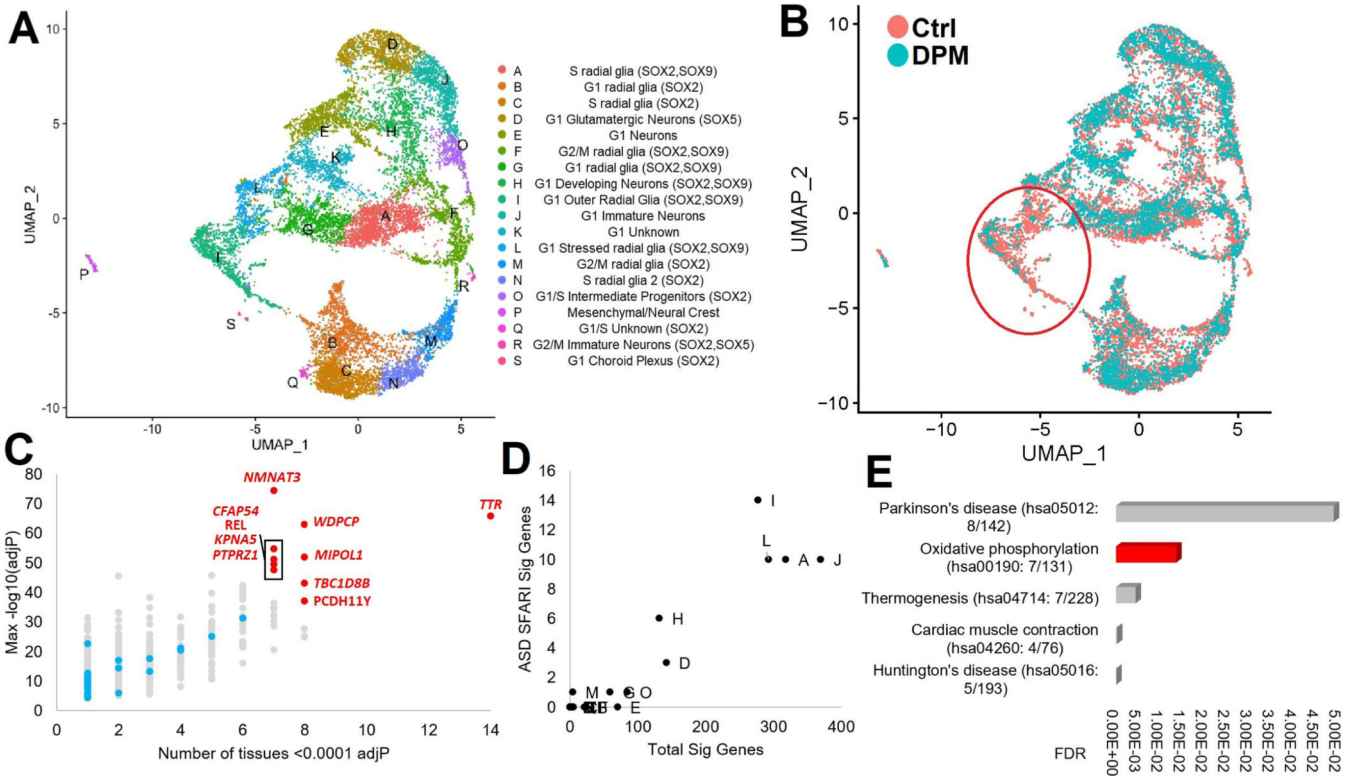

Fig. 4.

Single Cell (sc)RNAseq of control and DPM treated cerebral organoids. A). UMAP of cell expression (each dot) pooled from both control and DPM organoids identifying 19 cell clusters, labeled A-S with manually curated prediction of identifies. B) Comparison of DPM exposed vs control (Ctrl) cerebral organoids plotted as UMAP. Note the Outer radial glia cell clusters (group F) has a reduced number of cells in DPM exposed conditions (red circle). C) Significant genes of the DPM treatment shown as the highest -log10 adjusted Pvalue (y-axis) and the number of cell clusters that have an adjusted Pvalue <0.0001. Top ten genes are labeled in red. ASD SFARI genes are colored cyan. D) The number of significant genes in each cell cluster (x-axis) and the number of ASD genes significantly changed by DPM treatment. E) Top enriched KEGG pathways for genes found in ¾ of the group J, A, L, I.